


Article

Design of Promising Green Cation-Exchange-Membranes-Based Sulfonated PVA and Doped with Nano Sulfated Zirconia for Direct Borohydride Fuel Cells

Marwa H. Gouda ¹, Noha A. Elessawy ², Sami A. Al-Hussain ³ and Arafat Toghan ^{3,4,*}

¹ Polymer Materials Research Department, Advanced Technology and New Materials Research Institute (ATNMRI), City of Scientific Research and Technological Applications City (SRTA-City), Alexandria 21934, Egypt; marwagouda777@yahoo.com

² Computer Based Engineering Applications Department, Informatics Research Institute IRI, City of Scientific Research and Technological Applications City (SRTA-City), Alexandria 21934, Egypt; nony_essawy@yahoo.com

³ Chemistry Department, College of Science, Imam Mohammad Ibn Saud Islamic University (IMSIU), Riyadh 11623, Saudi Arabia; sahusain@imamu.edu.sa

⁴ Chemistry Department, Faculty of Science, South Valley University, Qena 83523, Egypt

* Correspondence: arafat.toghan@yahoo.com or aataahmed@imamu.edu.sa



Citation: Gouda, M.H.; Elessawy, N.A.; Al-Hussain, S.A.; Toghan, A. Design of Promising Green Cation-Exchange-Membranes-Based Sulfonated PVA and Doped with Nano Sulfated Zirconia for Direct Borohydride Fuel Cells. *Polymers* **2021**, *13*, 4205. <https://doi.org/10.3390/polym13234205>

Academic Editor: Cheng-Zhang Lu

Received: 31 October 2021

Accepted: 21 November 2021

Published: 30 November 2021

Publisher's Note: MDPI stays neutral with regard to jurisdictional claims in published maps and institutional affiliations.



Copyright: © 2021 by the authors. Licensee MDPI, Basel, Switzerland. This article is an open access article distributed under the terms and conditions of the Creative Commons Attribution (CC BY) license (<https://creativecommons.org/licenses/by/4.0/>).

Abstract: The direct borohydride fuel cell (DBFC) is a low-temperature fuel cell that requires the development of affordable price and efficient proton exchange membranes for commercial purposes. In this context, super-acidic sulfated zirconia (SO_4ZrO_2) was embedded into a cheap and environmentally friendly binary polymer blend, developed from poly(vinyl alcohol) (PVA) and iota carrageenan (IC). The percentage of SO_4ZrO_2 ranged between 1 and 7.5 wt.% in the polymeric matrix. The study findings revealed that the composite membranes' physicochemical features improved by adding increasing amounts of SO_4ZrO_2 . In addition, there was a decrease in the permeability and swelling ratio of the borohydride membranes as the SO_4ZrO_2 weight% increased. Interestingly, the power density increased to 76 mW cm^{-2} at 150 mA cm^{-2} , with 7.5 wt.% SO_4ZrO_2 , which is very close to that of Nafion117 (91 mW cm^{-2}). This apparent selectivity, combined with the low cost of the eco-friendly fabricated membranes, points out that DBFC has promising future applications.

Keywords: direct borohydride fuel cell; cation exchange membrane; poly(vinyl alcohol); iota carrageenan; sulfated zirconia

1. Introduction

One of the most important current global challenges is finding alternative solutions to conventional energy sources such as petroleum [1]. Recently, fuel cells (FCs) have been considered as sustainable energy sources, making them an attractive and alternative category to finite reserves [2–4]. They can directly convert chemical energy into electrical energy [5–9]

One of the different types of FCs that have been developed so far is the direct borohydride fuel cell (DBFC). It has a high-power density (HPD) at relatively low operating temperatures, which makes it a promising power system for portable applications [10,11]. In addition, it is fueled by non-explosive and non-toxic reactants, which enable it to be applied in the portable and transport sectors. The DBFC provides electrical power by reducing gaseous or liquid oxidants and oxidizing borohydride ions (BH_4^-). Sodium borohydride (NaBH_4) is utilized as a non-hydrocarbon liquid fuel; hence, there is no harmful emission of carbon dioxide compared to FCs fed with alcohol. In comparison to oxygen, liquid hydrogen peroxide (H_2O_2) is preferred as an oxidant due to its faster reduction

kinetics, which generate a higher power density. This broadens the application of DBFCs in oxygen-free environments, such as in space and in submarines [12–14].

A membrane is used as a separator in the fuel cell, between the anode and the cathode. It plays a vital role in ion transport to maintain the balance of charges in the cell. An anion-exchange membrane (AEM) easily transfers OH^- from cathode to anode. However, a cation-exchange membrane (CEM) is preferably used to separate the compartments of the cathode and anode in FCs. This is mainly because CEMs can better decrease the borohydride crossover compared to AEMs, due to the electrostatic repulsion that occurs between the negative charges of BH_4^- and the CEM [12]. In addition, CEMs help to transport Na^+ ions from the anode to the cathode. The Nafion family is widely used as perfluorinated CEMs in DBFCs [14–16], because it provides good chemical and mechanical stability, in addition to good ionic conductivity [12,14,15]. However, its membranes are very expensive and complicated in the manufacturing process, which limits its commercialization in fuel cells [17,18]. Due to this, it is very important to replace it with cheap, green polymeric membranes [12,14].

Non-perfluorinated polymers, such as poly(ether ether ketone) (PEEK), poly(benzimidazole) (PBI), poly(arylene ether sulfone) (PSU), and poly(styrene) (PS), are among the polymers most often used as alternatives [18–21]. However, synthesizing these non-degradable polymers takes time, generates harmful organic solvents, and uses high temperatures. These make the membrane synthesis complicated, costly, and not environmentally friendly. Therefore, researchers are looking for alternatives with green, efficient, and inexpensive polymeric films. Recently, the use of cheap, green polymers that can be biodegraded, such as polyvinyl alcohol (PVA) and iota carrageenan (IC), has become more attractive [18,22–25].

Thus, PVA is a well-suited polymer because it is chemically stable, can form film adhesion, and is hydrophilic [18,26,27]; however, its rigid, semi-crystalline structure gives it low proton conductivity. Due to this, it is seldom used as a proton-exchange membrane in FCs. Therefore, it is necessary to look for the possibility of repairing this defect. It has been found that adding dopants, or combining them with another polymer electrolyte, accomplishes this purpose [18,23,26]. For instance, PVA blended with functionalized titania [28], or sulfated/phosphated titania [29,30], enhances the membranes' ionic conductivity due to the formation of more hydrogen bonds. Furthermore, sulfonated graphene oxide was used as a doping agent in the same polymer matrix and achieved a power density of about $65 \text{ mW} \cdot \text{cm}^{-2}$ [31]. PVA blended with IC is favored due to hydrogen bond interactions between the $-\text{OH}$ groups of IC and PVA [32,33]. Moreover, IC is a commonly used biopolymer in synthesizing polymer electrolyte membranes [34] due to its non-toxic properties, chemical stability, and flexibility.

To improve the oxidative stability and the mechanical, thermal, and dimensional characteristics of the membrane, as well as its ability to hinder BH_4^- crossover and conduct ions, many researchers have commonly used a strategy such as inserting dopants into polymer structures for the production of a nanocomposite membrane [17,18,35,36]. Incorporation of sulfated zirconia (SO_4ZrO_2) into a polymer matrix is particularly beneficial in fuel cell applications because it is chemically stable, has a large surface area, is mechanically strong, and prevents fuel crossover [37–43]. SO_4ZrO_2 consists of hydrophilic functional groups that contain oxygen, such as sulfate groups. They can enhance water adsorption, thereby creating pathways for conducting protons [17,19,20]. When SO_4ZrO_2 is inserted into a polymer matrix, hydrogen bonds are formed between the oxygenated groups and $-\text{OH}$ groups of the polymer chains in SO_4ZrO_2 . These hydrogen bonds compress and strengthen the membrane matrix, preventing excessive water absorption and swelling [26,44,45]. In addition, the nanocomposite has more ability to conduct ions. This is as a result of the increased number of proton delivery sites, due to the presence of sulfate radicals in the structure of the nanocomposite.

In this respect, the current work aims to fabricate and develop a new SPVA/IC/ SO_4ZrO_2 membrane that fulfills the above requirements, to take a step forward towards commercializing DBFCs. To achieve this, SO_4ZrO_2 was first synthesized and then added as a dopant

into the matrix of SPVA/IC polymers at various concentrations. It led to the formation of a novel nanocomposite membrane called S-PVA/IC/SO₄ZrO₂. The oxygen groups of SO₄ZrO₂, including sulfate groups, are connected to the –OH groups of IC and PVA by generating hydrogen bonds, which are expected to improve the ability of the membrane to stabilize oxidation, conduct Na⁺, improve mechanical resistance, and hinder BH₄[−] crossover while reducing the absorption of excess water. The performance of the DBFC can be improved with the use of such a membrane.

2. Materials and Methods

2.1. Synthesis

2.1.1. Synthesis of Nano Sulfated Zirconia (SO₄ZrO₂)

SO₄ZrO₂ nanoparticles were prepared by simple calcination [46] of ammonium sulfate (NH₄)₂SO₄ and zirconium oxychloride octahydrate ZrOCl₂·8H₂O, with a 6:1 molar ratio, without any solvent. The powder mixture was calcined at 600 °C for 5 h, and then ground in ball mill.

2.1.2. Preparation of SPVA/IC/SO₄ZrO₂ Membranes

Ten grams of PVA (99% hydrolysis and medium mW, USA) was dissolved in 100 mL of deionized H₂O at 90 °C for 2 h. Two grams of IC (type V) was dissolved in 100 mL of deionized H₂O at 80 °C for 1 h. PVA: IC (95:5) wt.% was blended. Then, the polymer blend was crosslinked, using 5 g of glutaraldehyde (GA) (Alfa Aesar; 50 wt.% in H₂O) as a covalent crosslinker, and 5 g of 4-sulfophthalic acid (SPA) (Sigma-Aldrich; 99.9 wt.% in H₂O) as an ionic crosslinker and sulfonating agent for PVA [24,26]. Then, the inorganic–organic nanocomposite was prepared by incorporating 1, 2.5, 5, and 7.5 wt.% of SO₄ZrO₂ into the polymeric matrix. Figure S1, in Supplementary Materials, explains the S-PVA/IC/SO₄ZrO₂ membrane structure, within which PVA and IC are ionically crosslinked through the esterification reaction between the carboxylic groups of the sulfophthalic acid and the hydroxyl groups of the polymers. In addition, the acetal reactions between the hydroxyl groups of the polymers and the aldehyde groups of the glutaraldehyde led to the covalent crosslinking of the two polymers. Furthermore, there was the formation of hydrogen bonds between the oxygen-containing SO₄ZrO₂ groups and the –OH groups of the PVA and IC [33], respectively.

2.2. Characterization

For different samples, after being dried in airflow at room temperature, different tools were used to investigate their properties; a Fourier transform infrared spectrophotometer was used to record the FT-IR spectra (Shimadzu FTIR-8400 S, Shimadzu, Kyoto, Japan), while an X-ray diffractometer was used to evaluate the structures (Shimadzu 7000, Shimadzu, Kyoto, Japan). To trace the thermal characterization of the S-PVA/IC/SO₄ZrO₂ membranes, a thermo-gravimetric analyzer (Shimadzu TGA-50, Japan) and a differential scanning calorimeter (DSC) (Shimadzu DSC-60, Japan) were used, and the measurements were carried out under a nitrogen flow of 40 cm³·min^{−1} over a temperature range between room temperature and 800 °C. A scanning electron microscope (SEM) (Joel Jsm 6360LA-Japan) displayed the morphology of the membrane surface, while transmission electron microscopy (TEM, JEM 2100 electron microscope) was used to display the morphology of SO₄ZrO₂ nanoparticles. X-ray photoelectron spectroscopy (XPS), with a Phi 5300 ESCA system (Perkin-Elmer, Waltham, WA, USA), was used to investigate the elemental composition of SO₄ZrO₂ nanoparticles.

To evaluate the hydrophilicity of the membrane, there was measurement of the contact angle between the membrane surface and the water droplet, using a contact-angle analyzer (Rame-Hart Instrument Co.: Succasunna, NJ, USA, model 500-FI).

The measurement and calculation of the composite membranes' swelling ratio (SR) and water uptake (WU) are, respectively, shown in Equations (1) and (2), after the sample

(1 cm × 1 cm) was left in water overnight, then dried, using tissue to wipe away the surface moisture, and then rapidly weighed [47,48].

$$SR(\%) = \frac{L_{wet} - L_{dry}}{L_{dry}} \times 100 \quad (1)$$

$$WU(\%) = \frac{W_{wet} - W_{dry}}{W_{dry}} \times 100 \quad (2)$$

where L_{dry} and L_{wet} represent the length of dry and wet composite membranes, while W_{dry} and W_{wet} are the weight of dry and wet composite membranes, respectively.

Acid-base titration was used to determine the ion exchange capacity (IEC). The weighted samples were placed in 50 cm³ of a 2 M NaCl solution for two days, after which titration was completed with a 0.01 N NaOH solution. IEC was calculated as follows [29]:

$$IEC(\text{meq/g}) = \frac{V_{\text{NaOH}} \times C_{\text{NaOH}}}{W_d} \times 100 \quad (3)$$

where C_{NaOH} , V_{NaOH} , and W_d are sodium hydroxide solution concentration, the amount of sodium hydroxide used in titration, and the dry sample weight, respectively.

The dry nanocomposite membranes were put through a tensile strength test at room temperature until they disintegrated. Lloyd Instrument LR10k was used [29].

The membrane of the nanocomposite was placed vertically between two small tanks of 100 mL each in a glass diffusion chamber to test its borohydride permeability. An amount of 1 M NaBH₄ was poured into the donor tank (A), containing 4 M NaOH solution, which is a common DBFC anolyte. Water was poured inside the receptor tank (B) [29]. Borohydride diffused from A to B across the composite membrane, and the amounts of boron from the BH₄⁻ ions transported to tank (B) were measured using an inductively-coupled plasma atomic emission spectrophotometer (ICP-AES, model Prodigy, Teledyne Leeman Labs) every 2 h, four times. Equation (4) [29] was used to determine the borohydride crossover from A to B with time:

$$C_B(t) = \frac{A}{V_B} \frac{P}{L} C_A(t - t_0) \quad (4)$$

where A (cm²) is the diffusion area, V_B (cm³) is the receptor tank volume, L (cm) is the membrane thickness, C_B and C_A (mol·L⁻¹) are the borohydride concentrations in tanks B and A, respectively, the interval $(t - t_0)$ is the time of the BH₄⁻ crossover, and P is the BH₄⁻ permeability of the membrane (cm²·s⁻¹).

The selective nature of the membranes (the ratio of ionic conductivity to borohydride permeability) was determined because it can provide crucial information about the fuel cell's performance.

The oxidative stability of the membranes produced was determined using the nanocomposite membranes' weight loss (1.5 × 1.5 cm²) in Fenton's reagent (3 wt.% H₂O₂ consisting of 2 ppm FeSO₄) at 68 °C for 24 h [28].

The electrochemical impedance spectroscopy (EIS) approach was utilized to assess the ionic conductivity of the nanocomposite membranes. A PAR 273A potentiostat (Princeton Applied Research, Inc.: Oak Ridge, TN, USA), connected to a SI 1255 HF frequency response analyzer (FRA, Schlumberger Solartron), was used for this analysis. The membranes were dipped in a 4 M NaOH solution at room temperature for 30 min. [27,29,31]. They were then kept between two stainless steel electrodes at an open circuit potential of 5 mV, with a signal amplitude in the range of 100 Hz to 100 kHz. The ability of the membranes to conduct ions was determined using Equation (5) [28]:

$$\sigma = \frac{d}{RA} \quad (5)$$

where σ ($\text{S}\cdot\text{cm}^{-1}$) is the ionic conductivity of membrane, R (Ω) is the membrane resistance, A (cm^2) is the membrane area, and d (cm) is the membrane thickness.

The composite membranes were kept in a 0.5 M NaCl solution for one day, and then pre-activated in 2 M NaOH for 4 h to assess their DBFC performance [29]. A membrane with an active area of 50 cm^2 was used to separate the sides of two fuel cells, vertically, and the performance experiment was conducted in potentiostatic mode at room temperature. For the sake of comparison, Nafion 117 was utilized as a commercial reference membrane.

3. Results and Discussion

3.1. Characterization of SO_4ZrO_2 and Nanocomposite Membranes

Figure 1a shows the FTIR spectra of SO_4ZrO_2 . A wide peak of about 3400 cm^{-1} was observed, in addition to the peak at around 1630 cm^{-1} . This could be due to the adsorbed H_2O molecules, as well as the peak around 500 cm^{-1} , referred to as the Zr–O band. In the region of $1200\text{--}900 \text{ cm}^{-1}$, the SO_4^{2-} group IR bands were observed [49] with peaks at 1217, 1128, and 1016 cm^{-1} , which are characteristic of S–O. The bands at 950 and 1100 cm^{-1} can be attributed to the sulfate groups of doping agents. For the membranes, however, the bands around 3250 cm^{-1} are due to the hydroxyl groups, where H-bonding has a large influence on these bands in PVA and IC. The bands at 1600 cm^{-1} refer to the O–H bonds from water molecules. Their adsorption increases with increasing amounts of sulfated zirconia, due to its hydrophilic properties. The bands at about 2840 and 2300 cm^{-1} were due to the C–H bonds in the structure of the polymers [28], and the characteristic peak for iota carrageenan sulfate groups was seen at 830 cm^{-1} . The weak bands at 1700 and 1750 cm^{-1} corresponded to C=O bonds and C–H bonding in the aromatic structure of sulfophthalic acid (SPA), respectively. This demonstrates that the crosslinking process has been completed. As shown in Figure 1b, the amorphous structure of the synthesized membranes grew as the dopant concentration rose, indicating sufficient membrane capacity for excellent ion conduction [50]. However, the sulfated-zirconia-powder curve exhibited typical peaks intensity of SO_4ZrO_2 at a 2θ of 28,38,54. [38,51].

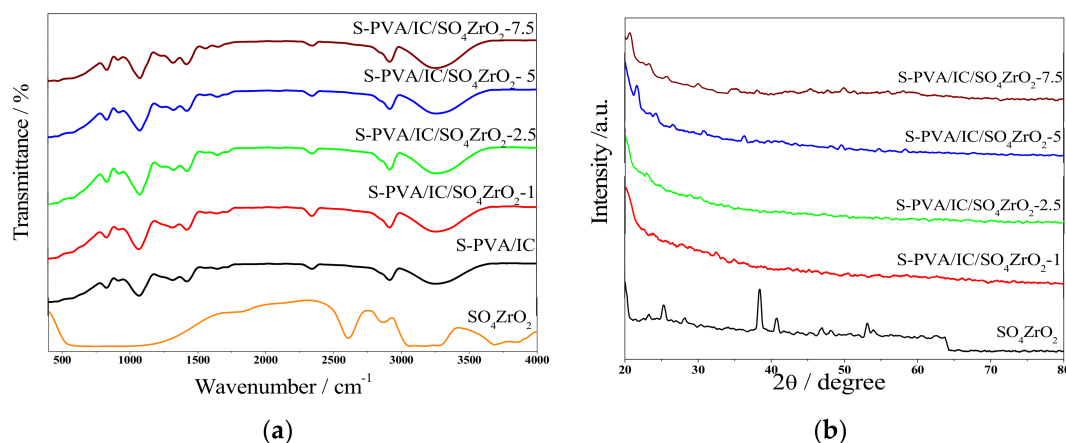


Figure 1. (a) FTIR spectra and (b) XRD patterns of SO_4ZrO_2 and S-PVA/IC/ SO_4ZrO_2 membranes.

Figure 2a,b shows that the surface of the undoped crosslinked membrane had no defects, while for the doped membrane, there was a good dispersion, without agglomeration, of sulfated zirconia. The TEM image in Figure 2c demonstrates that the sulfated zirconia formed nanoscale particles with a small concentration of aggregation. However, XPS elemental analysis was employed to confirm the synthesis of sulfated zirconia, as shown in Figure 3a, where sulfur groups were presented on the surface of SO_4ZrO_2 . In Figure 3b, the S2p spectrum of the sulfate group can be fitted into two major peaks, at 168.9 and 170.0 eV, assigned to S $2p_{3/2}$ and S $2p_{1/2}$ spectra for the oxidized sulfur species, respectively, while the Zr 3d spectrum shown in Figure 3c can be fitted into doublet peaks

at approximately 183.4 and 185.8 eV, corresponding to contributions from Zr 3d_{5/2} and Zr 3d_{3/2}, respectively.

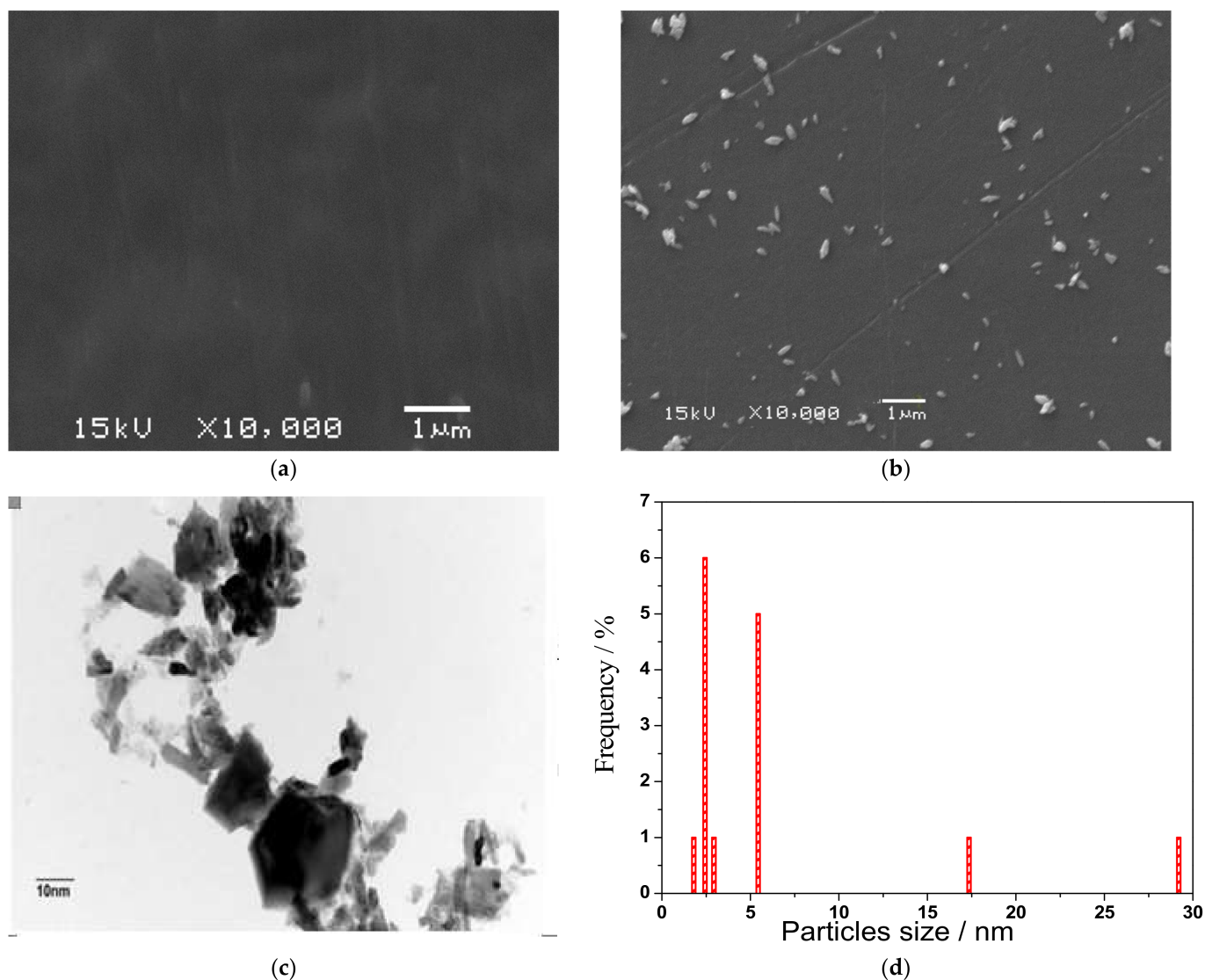


Figure 2. SEM images for (a) the undoped membrane surface and (b) the S-PVA/IC/SO₄ZrO₂-7.5 membrane surface; (c) TEM image for SO₄ZrO₂ nanoparticles and (d) frequency distribution plot of SO₄ZrO₂ nanoparticles size.

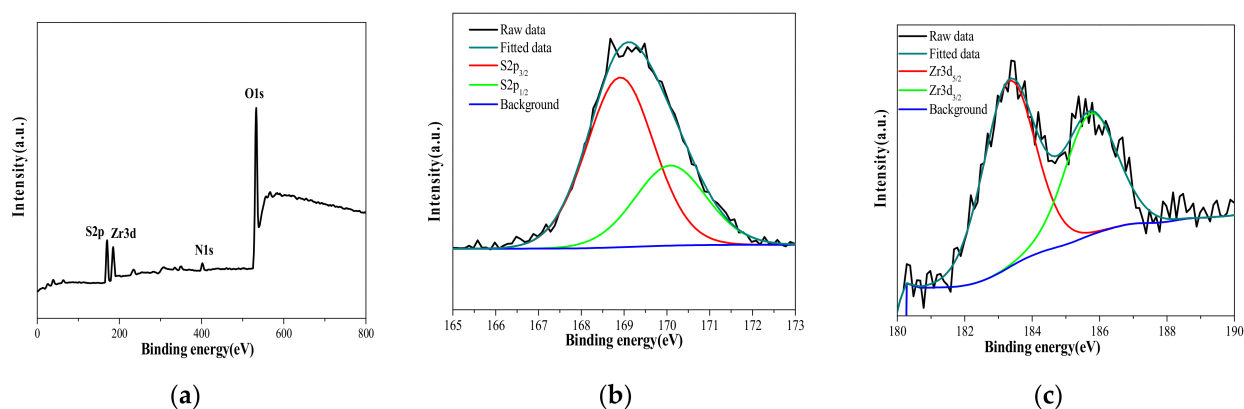


Figure 3. (a) XPS survey spectra of SO₄ZrO₂, (b) S2p spectra, and (c) Zr3d spectra of the synthesized SO₄ZrO₂ nanoparticles.

3.2. Thermal and Mechanical Analysis

Figure 4a depicts the TGA curves of polymeric blend membranes without and with SO_4ZrO_2 . The initial weight loss at approximately 150 °C (8%) is because the moisture evaporated in all membranes [23,52]. The second weight loss of composite membranes happened between 150 and 270 °C, due to the breakdown of functional groups [53,54]. The third weight-loss stage is characterized by a noteworthy breakdown from 270 to 360 °C. This could be attributed to the polymeric chain decomposition [52,55], which began at 230 °C for the undoped membranes, and at 270 °C, with a lower weight percentage, for doped membranes. This behavior demonstrates that the addition of a dopant compound to a composite membrane improves its thermal stability by boosting its covalent, ionic, and hydrogen bonding. Only one endothermic peak in DSC (Figure 3b) indicates complete miscibility of SO_4ZrO_2 in the membrane structure, and the absence of this peak at SO_4ZrO_2 , with a weight percent of 7.5, could be because many hydrogen bonds were formed between the dopant and the polymer structure. This partially destroyed its crystallinity [32,33], leading to a decrease in the membranes' melting temperature.

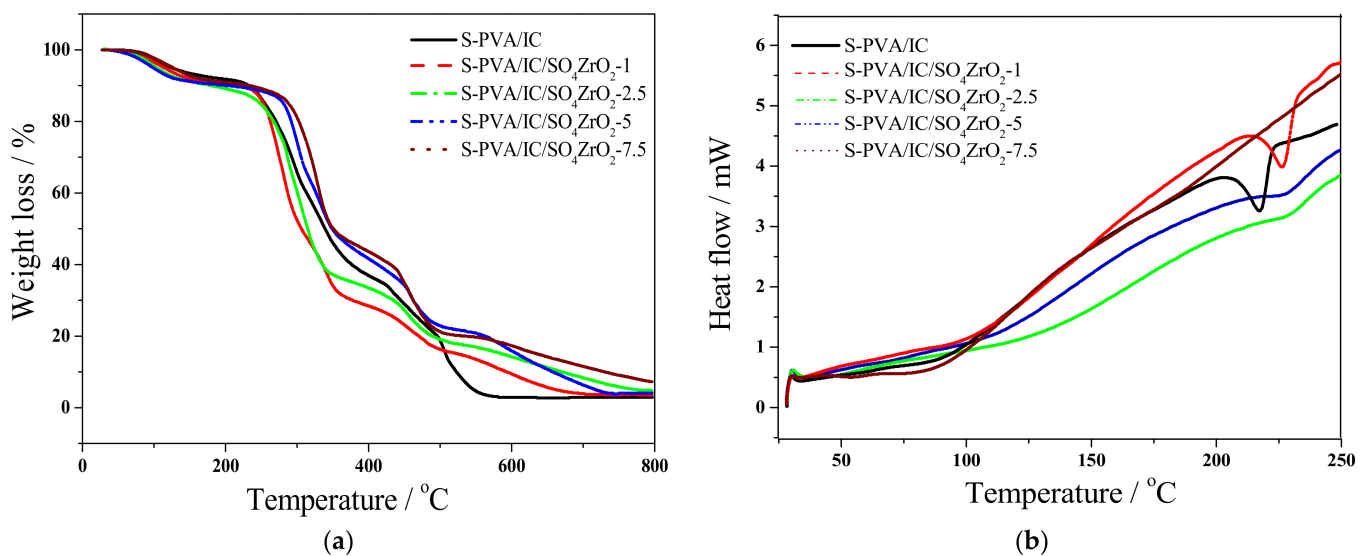


Figure 4. (a) TGA and (b) DSC curves of nanocomposite membranes.

The addition of SO_4ZrO_2 to the polymeric matrix enhances its mechanical tensile strength [51]. As shown in Figure 5, increasing the incorporation of SO_4ZrO_2 into the polymeric matrix increased the tensile strength of the nanocomposite membranes. This is due to the increase in the compatibility of the composite membrane, by increasing the connection between functional groups, such as SO_4^- and OH groups, as well as the characteristic groups of SO_4ZrO_2 , of the two polymers, via the formation of hydrogen, ionic, and covalent bonds. These bonds improved the nanocomposite membranes' interfacial adhesion in comparison to the membranes that were not doped.

Membrane surfaces are hydrophobic when contact angles are below 90°, and hydrophilic when they are more than 90°. The number of water molecules responsible for proton transport in the membrane must be measured; however, the membrane's ability to absorb more water promotes swelling, which reduces the membrane's mechanical strength. On the other hand, a lack of water molecules reduces the membrane's conductivity. This means the conductivity and strength of the membrane have an impact on fuel cell performance. Figure 5 shows the character of the manufactured composite membranes placed in deionized water. It shows that, as the composition of the dopant increased from 1 to 7.5 wt.%, the composite membranes became less hydrophilic and very thick [31,45]. In addition, the swelling ratio and water uptake of the polymeric membranes were reduced, which is highly important [56]. In other words, in comparison to the undoped membrane, an

increase in the dopant in the membrane matrix would increase the structure compactness. This prevents excess water in the pathways of the polymeric matrix [57–60].

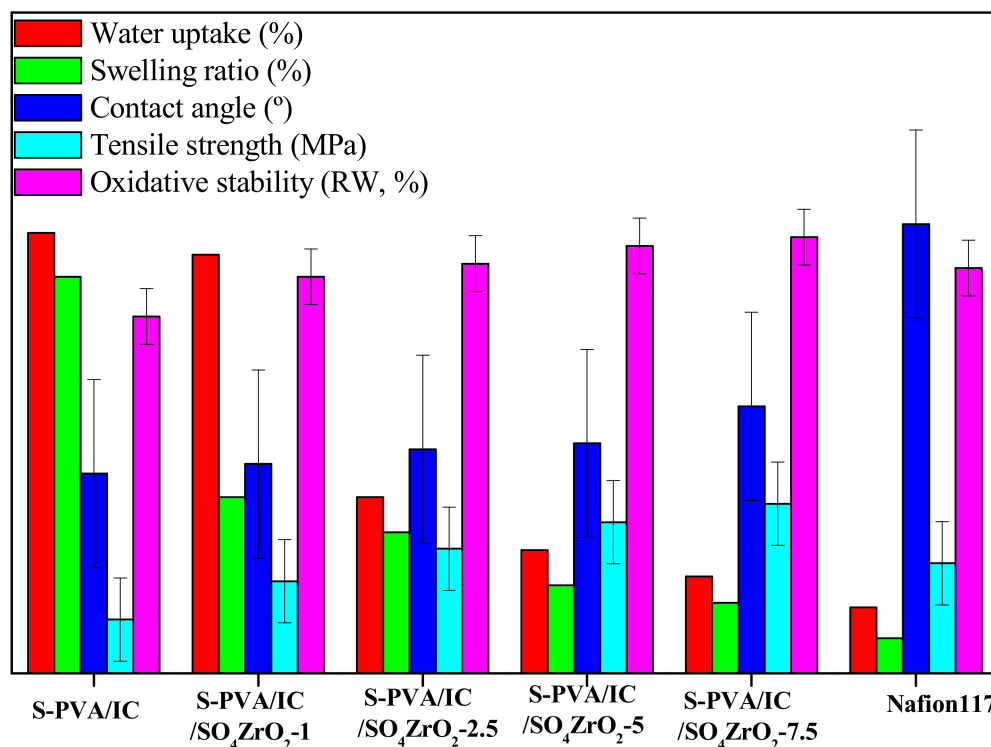


Figure 5. Physicochemical properties of the fabricated membranes and Nafion 117.

3.3. Oxidative Stability

Fenton's reagent test was utilized to determine the chemical stability of the composite membranes. As shown in Figure 5, the chemical stability of the undoped membrane was the lowest, but when SO_4ZrO_2 was added as a doping agent, the membranes' resistance to OOH and OH radical attack was improved. The most stable synthesized membrane was S-PVA/IC/ SO_4ZrO_2 -7.5. It maintained its weight at about 99%, demonstrating that adding SO_4ZrO_2 to the polymeric matrix increases its chemical stability [42].

3.4. Ionic Conductivity, IEC, and Borohydride Crossover

The ion exchange capacities of the doped and undoped membranes were compared to Nafion 117, as shown in Figure 6. The IEC values, represented in Table S2 in Supplementary Materials, increased as the volume of SO_4ZrO_2 in the composite membranes increased. This is because the composite membranes have more acidic exchangeable groups, which increases the charge in the polymeric matrix. Accordingly, the ionic conduction should be improved [45]. For instance, the S-PVA/IC/ SO_4ZrO_2 -7.5 membrane had higher ionic conductivity ($21.6 \text{ mS}\cdot\text{cm}^{-1}$) than the undoped membrane ($8.1 \text{ mS}\cdot\text{cm}^{-1}$), as shown in Figure S2 in Supplementary Materials.

For the fuel permeability of the composite membranes, as shown in Figure 6, it is clear that, by adding SO_4ZrO_2 to the polymeric matrix, the fuel permeability decreased. This is because the dopant can constrict the polymeric matrix channels and reduce water uptake, thus decreasing the BH_4^- permeability [29,31]. However, the higher selectivity of the S-PVA/IC/ SO_4ZrO_2 -7.5 membrane, which is $1.14 \times 10^5 \text{ mS}\cdot\text{cm}^{-3}$, as compared to the undoped S-PVA/IC membrane, which has a selectivity of around $0.25 \times 10^5 \text{ mS}\cdot\text{cm}^{-3}$, confirmed that the nanocomposite membranes produced are suitable for use in DBFCs [58].

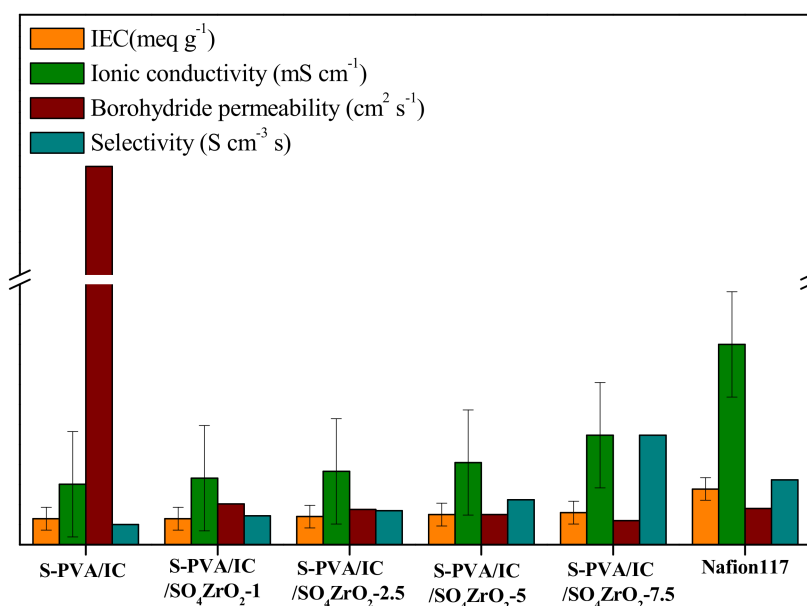


Figure 6. Ion exchange capacity, ionic conductivity, borohydride permeability, and selectivity of the fabricated membranes and Nafion 117.

3.5. Fuel Cell Performance

As shown in Figure 7a, the performance of the nanocomposite membrane S-PVA/IC/SO₄ZrO₂-7.5, which had the highest conductivity and lowest permeability, was tested in a lab DBFC, and compared to that of the Nafion 117[®] membrane using similar tests. The polarization curves reveal that the S-PVA/IC/SO₄ZrO₂-7.5 membrane resulted in lower DBFC discharge currents than Nafion117, because Nafion117 has a higher charge density. In addition, this could be due to electrochemical reactions at the anode and cathode that were restricted by Na⁺ ions' mass transfer via the S-PVA/IC/SO₄ZrO₂-7.5 membrane [29,31]. Furthermore, for an inside view of S-PVA/IC/SO₄ZrO₂-7.5 membrane stability, the same tested membranes were also subjected to a 48 h stability test, as shown in Figure 7b. The behavior of both DBFCs was similar for the first 30 h, but after that, the cell voltage of the DBFC with the Nafion117 membrane remained nearly stable, while the cell voltage of the DBFC with S-PVA/IC/SO₄ZrO₂-7.5 was reduced. This could be attributed to ohmic losses caused by the increase in the composite membranes' resistance.

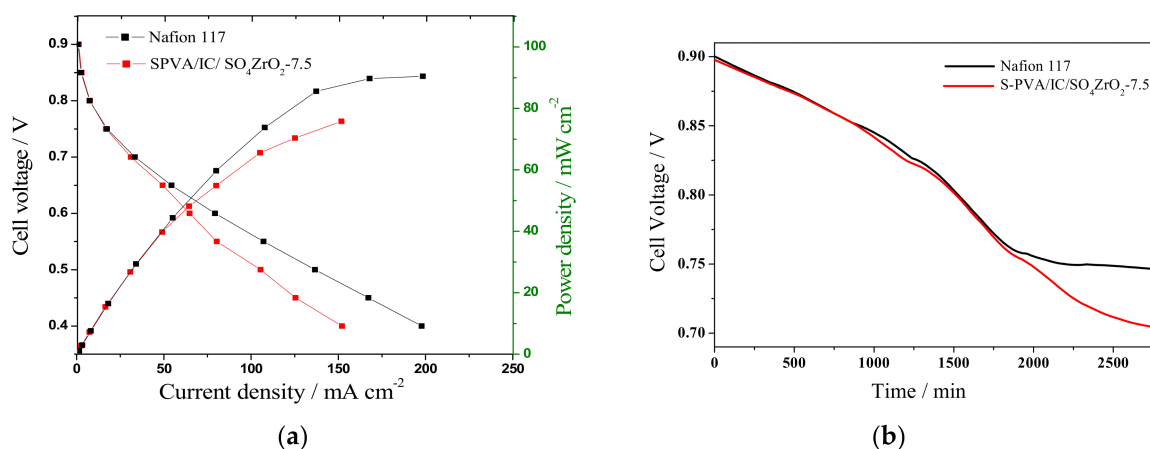


Figure 7. (a) Power density curves and polarization of DBFCs, and (b) fuel cell stability recorded at a current density of 50 mA·cm⁻² for 48 h, at room temperature, using PVA/IC/SO₄ZrO₂-7.5 and Nafion117 membranes.

4. Conclusions

Low-cost nanocomposite membranes were created using a simple blending and solution-casting method with environmentally friendly polymers. The incorporation of SO_4ZrO_2 as a dopant into the polymeric blend appears to improve the characteristics of the membrane, such as its mechanical stability, ionic conductivity, and oxidative stability, as well as its ability to reduce excess water and prevent BH_4^- crossover, particularly in the nanocomposite membrane with 7.5wt.% SO_4ZrO_2 . However, under the same experimental conditions, the S-PVA/IC/ SO_4ZrO_2 -7.5 membrane had a slightly lower peak power density, of about $76 \text{ mW}\cdot\text{cm}^{-2}$, than Nafion 117, which is $91 \text{ mW}\cdot\text{cm}^{-2}$. In addition, the S-PVA/IC/ SO_4ZrO_2 -7.5 membrane had good membrane stability in DBFCs, and could outperform Nafion 117 in terms of oxidative stability, tensile strength, and BH_4^- permeability. Moreover, it can commercially compete with Nafion117 due to its eco-friendly raw materials, low cost, and simple, green synthesis with no toxic solvents involved; it can also be easily manufactured industrially. For all previous reasons, the synthesized S-PVA/IC/ SO_4ZrO_2 -7.5 membrane can be utilized as PEM, after some modifications in its structure, to compete with Nafion 117 in all properties.

Supplementary Materials: The following are available online at <https://www.mdpi.com/article/10.3390/polym13234205/s1>. Figure S1: Possible structure of the S-PVA/ IC/ SO_4ZrO_2 membrane. Figure S2: Nyquist plot of S-PVA/IC and S-PVA/IC/ SO_4ZrO_2 nanocomposite membranes. Table S1: Physicochemical properties of the fabricated membranes and Nafion 117. Table S2: Ionic conductivity, Borohydride permeability, IEC and selectivity of the fabricated membranes and Nafion 117.

Author Contributions: Data curation, A.T.; Formal analysis, M.H.G., N.A.E. and A.T.; Funding acquisition, S.A.A.-H. and A.T.; Investigation, M.H.G., N.A.E. and A.T.; Methodology, M.H.G., N.A.E. and A.T.; Resources, S.A.A.-H.; Supervision, A.T.; Validation, M.H.G., N.A.E. and S.A.A.-H.; Writing—original draft, M.H.G., N.A.E. and A.T.; Writing—review & editing, M.H.G., N.A.E., S.A.A.-H. and A.T. All authors have read and agreed to the published version of the manuscript.

Funding: This research was funded by the Deanship of Scientific Research, Imam Mohammad Ibn Saud Islamic University, Saudi Arabia, Research Group no. RG-21-09-78.

Institutional Review Board Statement: Not applicable.

Informed Consent Statement: Not applicable.

Data Availability Statement: Not applicable.

Acknowledgments: The authors extend their appreciation to the Deanship of Scientific Research at Imam Mohammad Ibn Saud Islamic University, Saudi Arabia, for funding this research work through the Research Group no. RG-21-09-78.

Conflicts of Interest: The authors have no conflict to declare, and the funders had no role in the design of the study; in the collection, analyses, or interpretation of data; in the writing of the manuscript, or in the decision to publish the results.

References

1. He, G.; Ling, Y.; Jiang, H.; Toghan, A. Barium Titanate as a Highly Stable Oxygen Permeable Membrane Reactor for Hydrogen Production from Thermal Water Splitting. *ACS Sustain. Chem. Eng.* **2021**, *9*, 11147–11154.
2. Liu, B.; Hu, B.; Du, J.; Cheng, D.; Zang, H.Y.; Ge, X.; Su, Z. Precise Molecular Level Modification of Nafion with Bismuth Oxide Clusters for High performance Proton Exchange Membranes. *Angew. Chem. Int. Ed.* **2021**, *133*, 6141–6150. [CrossRef]
3. Faisal, F.; Toghan, A.; Khalakhan, I.; Vorokhta, M.; Matolin, V.; Libuda, J. Characterization of thin CeO_2 films electrochemically deposited on HOPG. *Appl. Surf. Sci.* **2015**, *350*, 142–148. [CrossRef]
4. Braesch, G.; Wang, Z.; Sankarasubramanian, S.; Oshchepkov, A.G.; Bonnefont, A.; Savinova, E.R.; Ramani, V.; Chatenet, M. A high performance direct borohydride fuel cell using bipolar interfaces and noble metal-free Ni-based anodes. *J. Mater. Chem. A* **2020**, *8*, 20543–20552. [CrossRef]
5. Liang, M.; Liu, Y.; Xiao, B.; Yang, S.; Wang, Z.; Han, H. An analytical model for the transverse permeability of gas diffusion layer with electrical double layer effects in proton exchange membrane fuel cells. *Int. J. Hydrog. Energy* **2018**, *43*, 17880–17888. [CrossRef]

6. Liang, M.; Fu, C.; Xiao, B.; Luo, L.; Wang, Z. A fractal study for the effective electrolyte diffusion through charged porous media. *Int. J. Heat Mass Transf.* **2019**, *137*, 365–371. [[CrossRef](#)]
7. Gouda, M.H.; Tamer, T.M.; Mohy Eldin, M.S. A highly selective novel green cation exchange membrane doped with ceramic nanotubes material for direct methanol fuel cells. *Energies* **2021**, *14*, 5664. [[CrossRef](#)]
8. Gouda, M.H.; Elessawy, N.A.; Toghan, A. Development of effectively costed and performant novel cation exchange ceramic nanocomposite membrane based sulfonated PVA for direct borohydride fuel cells. *J. Ind. Eng. Chem.* **2021**, *100*, 212–219. [[CrossRef](#)]
9. Gouda, M.; Tamer, T.; Konsowa, A.; Farag, H.; Eldin, M.M. Organic-Inorganic Novel Green Cation Exchange Membranes for Direct Methanol Fuel Cells. *Energies* **2021**, *14*, 4686. [[CrossRef](#)]
10. Sanli, A.E.; Gordesel, M.; Yilmaz, E.S.; Ozden, S.K.; Gunlu, G.; Uysal, B.Z. Performance improvement in direct borohydride/peroxide fuel cells. *Int. J. Hydrog. Energy* **2017**, *42*, 8119–8129. [[CrossRef](#)]
11. Demirci, U.B.; Akdim, O.; Andrieux, J.; Hannauer, J.; Chamoun, R.; Miele, P. Sodium Borohydride Hydrolysis as Hydrogen Generator: Issues, State of the Art and Applicability Upstream from a Fuel Cell. *Fuel Cells* **2010**, *10*, 335–350. [[CrossRef](#)]
12. Ma, J.; Choudhury, N.A.; Sahai, Y. A comprehensive review of direct borohydride fuel cells. *Renew. Sustain. Energy Rev.* **2010**, *14*, 183–199. [[CrossRef](#)]
13. Ong, B.C.; Kamarudin, S.K.; Basri, S. Direct liquid fuel cells: A review. *Int. J. Hydrog. Energy* **2017**, *42*, 10142–10157. [[CrossRef](#)]
14. Merino-Jiménez, I.; León, C.P.; Shah, A.A.; Walsh, F.C. Developments in direct borohydride fuel cells and remaining challenges. *J. Power Source* **2012**, *219*, 339–357. [[CrossRef](#)]
15. Šljukić, B.; Morais, A.L.; Santos, D.M.F.; Sequeira, C.A.C. Anion-or cation-exchange membranes for $\text{NaBH}_4/\text{H}_2\text{O}_2$ fuel cells? *Membranes* **2012**, *2*, 478–492. [[CrossRef](#)] [[PubMed](#)]
16. Santos, D.; Sequeira, C. Effect of Membrane Separators on the Performance of Direct Borohydride Fuel Cells. *J. Electrochem. Soc.* **2011**, *159*, B126–B132. [[CrossRef](#)]
17. Pandey, R.P.; Shukla, G.; Manohar, M.; Shahi, V.K. Graphene oxide based nanohybrid proton exchange membranes for fuel cell applications: An overview. *Adv. Colloid Interface Sci.* **2017**, *240*, 15–30. [[CrossRef](#)] [[PubMed](#)]
18. Sun, C.Y.; Zhang, H.; Luo, X.D.; Chen, N. A comparative study of Nafion and sulfonated poly(ether ether ketone) membrane performance for iron-chromium redox flow battery. *Ionics* **2019**, *25*, 4219–4229. [[CrossRef](#)]
19. Ye, Y.-S.; Rick, J.; Hwang, B.-J. Water Soluble Polymers as Proton Exchange Membranes for Fuel Cells. *Polymers* **2012**, *4*, 913–963. [[CrossRef](#)]
20. Pourzare, K.; Farhadi, S.; Mansourpanah, Y. Advanced nanocomposite membranes for fuel cell applications: A comprehensive review. *Biofuel Res. J.* **2016**, *3*, 496–513. [[CrossRef](#)]
21. Akay, R.G.; Ata, K.C.; Kadioğlu, T.; Çelik, C. Evaluation of SPEEK/PBI blend membranes for possible direct borohydride fuel cell (DBFC) application. *Int. J. Hydrog. Energy* **2018**, *43*, 18702–18711. [[CrossRef](#)]
22. Ata, K.C.; Kadioğlu, T.; Türkmen, A.C.; Çelik, C.; Akay, R.G. Investigation of the effects of SPEEK and its clay composite membranes on the performance of Direct Borohydride Fuel Cell. *Int. J. Hydrog. Energy* **2020**, *45*, 5430–5437. [[CrossRef](#)]
23. Wei, Q.; Zhang, Y.; Wang, Y.; Chai, W.; Yang, M. Measurement and modeling of the effect of composition ratios on the properties of poly(vinyl alcohol)/poly(vinyl pyrrolidone) membranes. *Mater. Des.* **2016**, *103*, 249–258. [[CrossRef](#)]
24. Maarouf, S.; Tazi, B.; Guenoun, F. Preparation and characterization of new composite membranes containing polyvinylpyrrolidone, polyvinyl alcohol, sulfosuccinic acid, silicotungstic acid and silica for direct methanol fuel cell applications. *J. Mater. Environ. Sci.* **2017**, *8*, 2870–2876.
25. Pintauro, P.N. Perspectives on Membranes and Separators for Electrochemical Energy Conversion and Storage Devices. *Polym. Rev.* **2015**, *55*, 201–207. [[CrossRef](#)]
26. Choudhury, N.; Ma, J.; Sahai, Y. High performance and eco-friendly chitosan hydrogel membrane electrolytes for direct borohydride fuel cells. *J. Power Source* **2012**, *210*, 358–365. [[CrossRef](#)]
27. Chen, J.; Li, Y.; Zhang, Y.; Zhu, Y. Preparation and characterization of graphene oxide reinforced PVA film with boric acid as crosslinker. *J. Appl. Polym. Sci.* **2015**, *132*, 1–8. [[CrossRef](#)]
28. Ye, Y.S.; Cheng, M.Y.; Xie, X.L.; Rick, J.; Huang, Y.J.; Chang, F.C.; Hwang, B.J. Alkali doped polyvinyl alcohol/graphene electrolyte for direct methanol alkaline fuel cells. *J. Power Source* **2013**, *239*, 424–432. [[CrossRef](#)]
29. Gouda, M.H.; Elessawy, N.A.; Santos, D.M.F. Synthesis and Characterization of Novel Green Hybrid Nano-composites for Application as Proton Exchange Membranes in Direct Borohydride Fuel Cells. *Energies* **2020**, *13*, 1180. [[CrossRef](#)]
30. Gouda, M.H.; Gouveia, W.; El Essawy, N.A.; Šljukić, B.; Nassr, A.B.A.A.; Santos, D.M.F. Simple design of PVA-based blend doped with $\text{SO}_4(\text{PO}_4)$ -functionalised TiO_2 as an effective membrane for direct borohydride fuel cells. *Int. J. Hydrogen Energy* **2020**, *45*, 15226–15238. [[CrossRef](#)]
31. Gouda, M.; Gouveia, W.; Afonso, M.; Šljukić, B.; El Essawy, N.; Santos, D. Novel Ternary Polymer Blend Membranes Doped with $\text{SO}_4/\text{PO}_4\text{-TiO}_2$ for Low Temperature Fuel Cells. In Proceedings of the 5th World Congress on Mechanical, Chemical, and Material Engineering (MCM'19), Paper No. ICCPE 106. Lisbon, Portugal, 15–17 August 2019. [[CrossRef](#)]
32. Gouda, M.; Gouveia, W.; Afonso, M.; Šljukić, B.; El Essawy, N.; Nassr, A.; Santos, D. Poly (vinyl alcohol)-based crosslinked ternary polymer blend doped with sulfonated graphene oxide as a sustainable composite membrane for direct borohydride fuel cells. *J. Power Source* **2019**, *432*, 92–101. [[CrossRef](#)]

33. Mohy Eldin, M.S.; Farag, H.A.; Tamer, T.M.; Konsowa, A.H.; Gouda, M.H. Development of novel iota carrageenan-g-polyvinyl alcohol polyelectrolyte membranes for direct methanol fuel cell application. *Polym. Bull.* **2020**, *77*, 4895–4916. [[CrossRef](#)]
34. Gouda, M.H.; Konsowa, A.H.; Farag, H.A.; Elessawy, N.A.; Tamer, T.M.; Mohy Eldin, M.S. Novel nanocomposite membranes based on cross-linked eco-friendly polymers doped with sulfated titania nano-tubes for direct methanol fuel cell application. *Nanomater. Nanotechnol.* **2020**, *10*, 1–9. [[CrossRef](#)]
35. Karthikeyan, S.; Selvasekarapandian, S.; Premalatha, M.; Monisha, S.; Boopathi, G.; Aristatil, G.; Arun, A.; Madeswaran, S. Proton-conducting I-Carrageenan-based biopolymer electrolyte for fuel cell application. *Ionics* **2016**, *23*, 2775–2780. [[CrossRef](#)]
36. Sedesheva, Y.S.; Ivanov, V.S.; Wozniak, A.I.; Yegorov, A.S. Proton-Exchange Membranes Based on Sulfonated Polymers. *Orient. J. Chem.* **2016**, *32*, 2283–2296. [[CrossRef](#)]
37. Awang, N.; Ismail, A.; Jaafar, J.; Matsuura, T.; Junoh, H.; Othman, M.H.D.; Rahman, M. Functionalization of polymeric materials as a high performance membrane for direct methanol fuel cell: A review. *React. Funct. Polym.* **2015**, *86*, 248–258. [[CrossRef](#)]
38. Sacca, A.; Gatto, I.; Carbone, A.; Pedicini, R.; Passalacqua, E. ZrO₂-Nafion composite membranes for polymer electrolyte fuel cells (PEFCs) at intermediate temperature. *J. Power Source* **2006**, *163*, 47–51. [[CrossRef](#)]
39. D'Epifanio, A.; Navarra, M.A.; Weise, F.C.; Mecheri, B.; Farrington, J.; Licocchia, S.; Greenbaum, S. Composite Nafion/Sulfated Zirconia Membranes: Effect of the Filler Surface Properties on Proton Transport Characteristics. *Chem. Mater.* **2009**, *22*, 813–821. [[CrossRef](#)]
40. Giffin, G.A.; Piga, M.; Lavina, S.; Navarra, M.A.; D'Epifanio, A.; Scrosati, B.; Di Noto, V. Characterization of sulfated-zirconia/Nafion[®] composite membranes for proton exchange membrane fuel cells. *J. Power Source* **2012**, *198*, 66–75. [[CrossRef](#)]
41. Navarra, M.; Abbati, C.; Scrosati, B. Properties and fuel cell performance of a Nafion-based, sulfated zirconia-added, composite membrane. *J. Power Source* **2008**, *183*, 109–113. [[CrossRef](#)]
42. Ren, S.; Sun, G.; Li, C.; Song, S.; Xin, Q.; Yang, X. Sulfated zirconia-Nafion composite membranes for higher temperature direct methanol fuel cells. *J. Power Source* **2006**, *157*, 724–726. [[CrossRef](#)]
43. Tominaka, S.; Momma, T.; Scrosati, B.; Osaka, T. Sulfated zirconia as a proton conductor for fuel cells: Stability to hydrolysis and influence on catalysts. *J. Power Source* **2010**, *195*, 4065–4071. [[CrossRef](#)]
44. Zhai, Y.; Zhang, H.; Hu, J.; Yi, B. Preparation and characterization of sulfated zirconia (SO₄²⁻/ZrO₂)/Nafion composite membranes for PEMFC operation at high temperature/low humidity. *J. Membr. Sci.* **2006**, *280*, 148–155. [[CrossRef](#)]
45. Deshmukh, K.; Ahamed, M.B.; Sadasivuni, K.K.; Ponnamma, D.; Deshmukh, R.R.; Pasha, S.K.K.; AlMaadeed, M.A.-A.; Chidambaram, K. Graphene oxide reinforced polyvinyl alcohol/polyethylene glycol blend composites as high-performance dielectric material. *J. Polym. Res.* **2016**, *23*, 1–13. [[CrossRef](#)]
46. Li, A.; Xiao, L.; Jiang, Z.; Tian, X.; Luo, L.; Liu, W.; Xu, Z.L.; Yang, H.; Jiang, Z.J. Sulfonic acid functionalized graphene oxide paper sandwiched in sulfonatedpoly (ether ether ketone): A proton exchange membrane with high performance for semi-passive direct methanol fuel cells. *Int. J. Hydrog. Energy* **2017**, *42*, 16731–16740. [[CrossRef](#)]
47. Sun, Y.; Ma, S.; Du, Y.; Yuan, L.; Wang, S.; Yang, J.; Deng, F.; Xiao, F. Solvent-Free Preparation of Nanosized Sulfated Zirconia with Brønsted Acidic Sites from a Simple Calcination. *J. Phys. Chem. B* **2005**, *109*, 2567–2572. [[CrossRef](#)] [[PubMed](#)]
48. Gouda, M.H.; Elessawy, N.A.; Toghan, A. Novel crosslinked sulfonated PVA/PEO doped with phosphated titanium oxide nanotubes as effective green cation exchange membrane for direct borohydride fuel cells. *Polymers* **2021**, *13*, 2050. [[CrossRef](#)] [[PubMed](#)]
49. Gouda, M.H.; Konsowa, A.H.; Farag, H.A.; Elessawy, N.A.; Tamer, T.M.; Eldin, M.S.M. Development novel eco-friendly proton exchange membranes doped with nano sulfated zirconia for direct methanol fuel cells. *J. Polym. Res.* **2021**, *28*, 1–10. [[CrossRef](#)]
50. Parnian, M.J.; Rowshanzamir, S.; Moghaddam, J.A. Investigation of physicochemical and electrochemical properties of recast Nafionnanocomposite membranes using different loading of zirconia nanoparticlesfor proton exchange membrane fuel cell applications. *Mater. Sci. Energy Technol.* **2018**, *1*, 146–154.
51. Yu, X.; Qiang, L. Preparation for Graphite Materials and Study on Electrochemical Degradation of Phenol by Graphite Cathodes. *Adv. Mater. Phys. Chem.* **2012**, *2*, 63–68. [[CrossRef](#)]
52. Mossayebi, Z.; Parnian, M.P.; Rowshanzamir, S. Effect of the Sulfated Zirconia Nanostructure Characteristics on Physicochemical and Electrochemical Properties of SPEEK Nanocompo-site Membranes for PEM Fuel Cell Applications. *Macromol. Mater. Eng.* **2018**, *303*, 1700570. [[CrossRef](#)]
53. Kowsari, E.; Zare, A.; Ansari, V. Phosphoric acid-doped ionic liquid-functionalized graphene oxide/sulfonated polyimide composites as proton exchange membrane. *Int. J. Hydrog. Energy* **2015**, *40*, 13964–13978. [[CrossRef](#)]
54. Bayer, T.; Cuning, B.V.; Selyanchyn, R.; Daio, T.; Nishihara, M.; Fujikawa, S.; Sasaki, K.; Lyth, S.M. Alkaline anion exchange membranes based on KOH-treated multilayer graphene oxide. *J. Membr. Sci.* **2016**, *508*, 51–61. [[CrossRef](#)]
55. Pandey, R.; Shahi, V. Sulphonatedimidized graphene oxide (SIGO) based polymer electrolyte membrane for improved water retention, stability and proton conductivity. *J. Power Source* **2015**, *299*, 104–113. [[CrossRef](#)]
56. Shirdast, A.; Sharif, A.; Abdollahi, M. Effect of the incorporation of sulfonated chitosan/sulfonated graphene oxide on the proton conductivity of chitosan membranes. *J. Power Source* **2016**, *306*, 541–551. [[CrossRef](#)]
57. Beydaghi, H.; Javanbakht, M.; Kowsari, E. Synthesis and Characterization of Poly(vinyl alcohol)/Sulfonated Graphene Oxide Nanocomposite Membranes for Use in Proton Exchange Membrane Fuel Cells (PEMFCs). *Ind. Eng. Chem. Res.* **2014**, *53*, 16621–16632. [[CrossRef](#)]

-
58. Qiu, X.; Dong, T.; Ueda, M.; Zhang, X.; Wang, L. Sulfonated reduced graphene oxide as a conductive layer in sulfonated poly(ether ether ketone) nanocomposite membranes. *J. Membr. Sci.* **2017**, *524*, 663–672. [[CrossRef](#)]
 59. Cheng, T.; Feng, M.; Huang, Y.; Liu, X. SGO/SPEN-based highly selective polymer electrolyte membranes for direct methanol fuel cells. *Ionics* **2017**, *23*, 2143–2152. [[CrossRef](#)]
 60. Luo, T.; Xu, H.; Li, Z.; Gao, S.; Fang, Z.; Zhang, Z.; Wang, F.; Ma, B.; Zhu, C. Novel proton conducting membranes based on copolymers containing hydroxylated poly(ether ether ketone) and sulfonated polystyrenes. *J. Appl. Polym. Sci.* **2017**, *134*, 1–8. [[CrossRef](#)]